



Research article

Numerical modeling and CFD simulation of diffuser augmented dual vertical axis hydrokinetic Banki-Michell turbine

Nebiyu Bogale Mereke^{a,b,*}, Venkata Ramayya Ancha^a, Patrick Hendrick^b^a Faculty of Mechanical Engineering, Jimma University Institute of Technology, Jimma, 378, Ethiopia^b Université Libre de Bruxelles, Aero-Thermo-Mechanics Department, Avenue F.D. Roosevelt 50, CP 165/41, 1050, Brussels, Belgium

ARTICLE INFO

Keywords:

Banki turbine
Hydrokinetic
Nozzle
Nozzle-diffuser
CFD

ABSTRACT

Hydrokinetic Banki turbines present an affordable, technically feasible, environmentally friendly technology. Their construction without requiring more expensive structures like diversion weirs, canals, forebay, and penstock, makes their initial investment much lower than commonly used horizontal Banki turbine of the same capacity. The possibility to install in the existing canals for Ultra Low Head applications is the additional motivating factor for this research. The system studied includes two Banki runners without internal shafts mounted vertically side by side surrounded by nozzle and diffuser structures. In the first scenario, Nozzle and then the Nozzle-diffuser augmented structures were separately studied to enhance the output of the runner for ultra-low head application, and the effects of each on the speed, pressure, and power output were analyzed. For the case of commonly used Banki, without nozzle and diffuser augmentation the speed for Ultra Low Head was minimum and determined to be 344 rpm, which is far below the recommended value of 800 rpm for safe operation at a flow rate of $1 \text{ m}^3/\text{s}$. In view of this, in the present study the enhanced speed on account of improvement was found to be 850 rpm and 1025 rpm for the design without and with diffuser assemblies respectively. Besides, the performance is seen to be improved by 7.6% with the diffuser as compared with the one without diffuser assembly. Detailed simulation results are presented and discussed: 3D ANSYS-FLUENT optimization result provided optimum number of blades for each runner to be 19 and with the optimum throat width in both cases as 202 mm. On account of the lack of any results reported so far for this innovative geometry, validation of the simulated results was carried out with reported results for the dual horizontal axis Banki turbines with good agreement.

1. Background

With so much potential for water resources, hydrokinetic energy, which may be obtained from the flow of water in irrigation and rainy channels, is a viable technology in developing nations like Ethiopia. In order to extract energy, stream flow systems often require a higher flow rate at low pressure; nevertheless, conventional hydraulic turbines perform better at high head and flow rates. In order to capture the most kinetic energy feasible, numerous studies have attempted to create novel and distinctive technological designs and configurations [1]. One potential solution for powering rural residents who live outside the reach of the grid is the use of hydrokinetic turbines, a recently developed renewable technology that is particularly new to the Ethiopian market. This makes it imperative to

* Corresponding author.

E-mail address: nbogale2015@gmail.com (N.B. Mereke).<https://doi.org/10.1016/j.heliyon.2024.e26970>

Received 16 September 2023; Received in revised form 20 February 2024; Accepted 22 February 2024

Available online 28 February 2024

2405-8440/© 2024 Published by Elsevier Ltd.

This is an open access article under the CC BY-NC-ND license

[\(http://creativecommons.org/licenses/by-nc-nd/4.0/\)](http://creativecommons.org/licenses/by-nc-nd/4.0/).

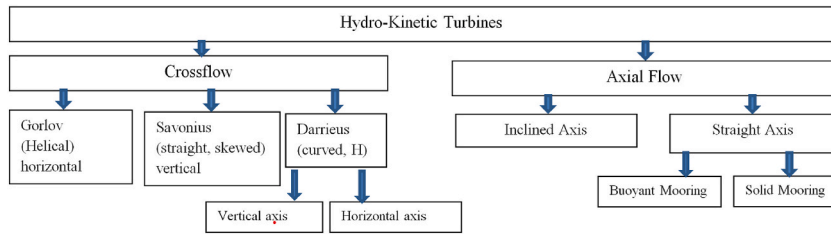


Fig. 1. Classification of hydrokinetic turbine rotors [1].

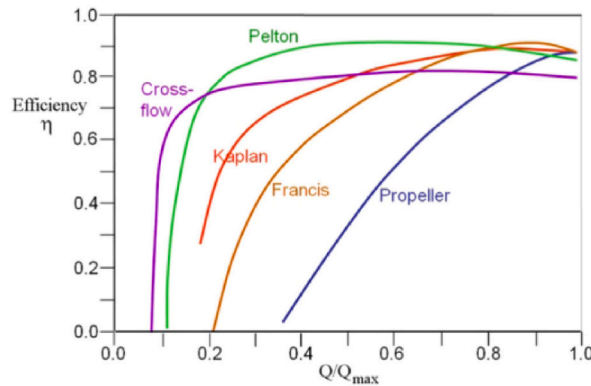


Fig. 2. Variation of efficiency with the percentage of maximum discharge (Sinagra et al., 2014).

conduct research on the Banki turbine that will be used as a hydrokinetic turbine with various geometric configurations [2]. Accordingly, dual vertical axis, cross-flow Banki turbines will be tested numerically in this study, along with CFD modelling using Ansys Fluent, and the results will be verified against recent studies on horizontal axis hydrokinetic Banki turbines.

1.1. Type and configuration of hydrokinetic turbine

Type and configuration depend on the type of resource in which the turbine is deployed. Through a wide literature search, hydrokinetic turbines can be classified into two broad categories as axial flow turbine and cross-flow turbine as shown in Fig. 1. The classification depends upon the alignment axis of rotation with respect to the water flow direction. Horizontal-axis turbines are mostly used in tidal energy extraction due to their higher efficiency. However, for generation of small-scale power, the vertical-axis turbine is usually preferred over the horizontal-axis turbine because of certain advantages such as design simplicity, independence of flow direction and ease of installation, lower maintenance cost as the electrical components can be installed above the free surface of the water [1]. For micro hydro power generation pump as turbine, propeller turbines could also be used, but considering their relative manufacturing difficulty and scarce availability Banki-Michell turbines are considered in this paper.

All the work so far have been studied on horizontal axis Banki turbine however no systematic investigation has been carried on vertical axis Banki which can be operated in hydrokinetic mode without the need for construction of civil, and mechanical structures like diversion weir, penstock etc., which requires more than 50% of the total cost of small hydropower system. This common Banki turbine system requires relatively large investment for the poor detached communities as compared with the vertical axis hydrokinetic Banki turbine studied in this research, therefore an affordable, easier to be manufactured, assembled and installed in existing irrigation, waterway systems where there is running water exists at low head studied. In addition removing inner shaft section and augmenting with nozzle diffuser geometries provide better performance for this new orientation of Banki turbine for ultra low head power generation.

In this research the first section, which is the background section, describes old and new ways of using Banki-Michell turbines, Why Banki-Michell turbines are good choice? And problem statement section. In section two based on latest design procedure for Banki-Michell turbine, the runner, distributor and diffuser designs performed and all detailed geometrical parameters fixed. Section three discusses about the numerical model to be used in Ansys-fluent after developing SolidWorks model. Section four discusses mesh refinement, geometry optimization, velocity triangle and degree of reaction. Section five discusses validation of results for both with and without diffuser designs. Section six discusses the results of the velocity, pressure, torque and power output. In addition, all the designs and different contour and velocity vectors developed. The final section draws conclusion.

Table 1
Conventional turbine-specific speed [5].

No	Turbine Type	Specific speed
1	Pelton and waterwheel	10–35
2	Francis	60–300
3	Cross-Flow	70–180
4	Kaplan dan propeller	300–1000

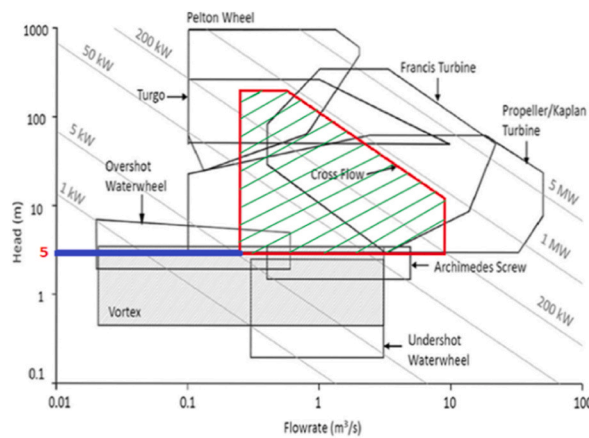


Fig. 3. Turbine selection chart cross flow turbine [5].

1.2. Why Banki-Michell is a good choice?

The installation of this technology can be done without a thorough site study in areas with irrigation canals, traditional water mills, waterways with controlled water discharge, water treatment plants, and power plants. It also has a relatively lower initial investment when compared to other hydropower technologies of similar capacity and less environment impact. The simpler manufacturing process of Banki turbines, which involves only cutting and welding in small, local workshops with limited equipment, and which even illiterate farmers can easily maintain, makes it very appealing to install Banki turbines in remote, hard-to-reach rural areas for Non-Interconnected Zones, particularly for developing countries. The cross-flow turbine is an ideal choice for producing energy without supervision because of its outstanding behavior with partial loads [3]. When examining several turbine performance characteristic curves, the Banki turbine exhibits consistent production despite variations in flow caused by seasonal fluctuations. Comparative analyses of 26 Banki turbines for 16 small hydropower plants in Bulgaria with heads between 22 and 142 m and powers up to 500 kW with a micro-Kaplan turbine of the same capacity reveal that Banki turbines are seven times less expensive.

Though the maximum efficiency is typically lower by a factor of 5–10 percent, the Banki turbine can guarantee an almost flat efficiency curve for a wider range of flow rates than the Francis turbine as shown in Fig. 2.

The lifespan is between forty and fifty years. Over its lifetime, the Banki turbine doesn't need a lot of maintenance. Its propensity for self-cleaning is another benefit. Losses are avoided because leaves, grass, etc., do not stay in the runner after the water exits it. Because of this, even though the turbine's efficiency is a little lower, it is more dependable than other kinds. Generally speaking, no runner cleaning is required, for example, due to flow inversion or speed changes. Some turbine types have higher nominal efficiencies, but they lose power more easily due to clogging.

It can also be applied to lower water distribution system pressure in areas where high water distribution network pressure damages pipes [4]. Furthermore, according to CINK Hydro-energy's technical specifications, Banki assembly the turbines' bearings are shielded from the flow by coatings and are simple to lubricate and regulate, which promotes longevity and ease of maintenance.

Although the geometric configuration of the Banki turbine studied in this research may yield good results for ultra-low head applications, as shown in Table 1 Banki turbine exhibits large specific speed and lower rotational speed for head lower than 5 m and provides poor performance.

Despite this, there is not enough research available for applications involving ultra-low head [2]. Elbatran et al. assembled two horizontal axis cross-flow turbines with the nozzle at the inlet and the diffuser at the outlet, creating what is known as a bi-directional diffuser augmented system, in order to study horizontal axis hydrokinetic turbines both numerically and experimentally. He also cites earlier research for turbine sizing, pointing out that there is a deficiency of theoretical knowledge regarding altering these angles to satisfy his hydrokinetic applications. The upper turbine may need to have its efficiency improved because the pressure and performance of the lower turbine are higher than those of the upper. In addition, the efficiency may be impacted by the flow control mechanism [2].

With the use of hydrokinetic turbines and no additional infrastructure—such as weirs, barrages, or falls—hydrokinetic is a novel

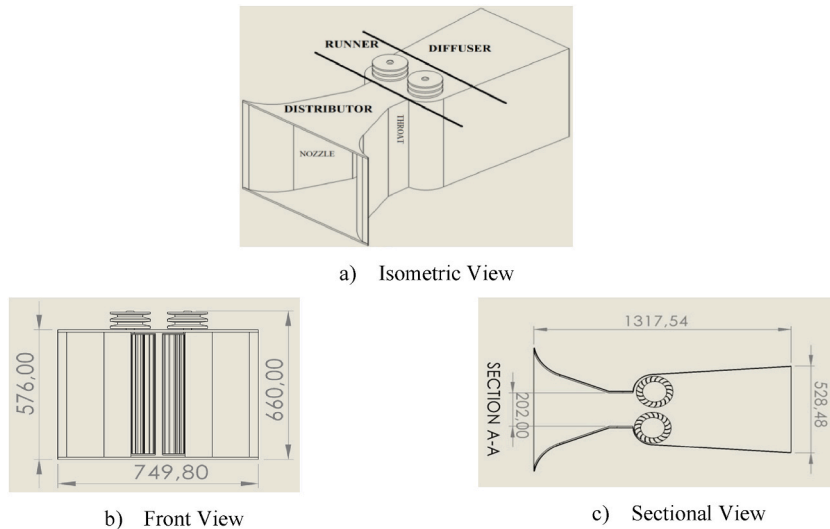


Fig. 4. New design arrangement for the study.

form of micro hydropower that captures the kinetic energy of water flowing through open channels, rivers, or canals [4].

Because nozzles can increase the harnessed power, they are the most efficient way to accelerate the flow. Nozzles can be ducted around turbines or used in micro channel flow streams. Furthermore, a number of studies have looked into CFD and experimental results of performance augmentation obtained by enclosing wind and hydrokinetic turbines in different-shaped diffusers. These studies come to the conclusion that a ducted turbine should be able to extract more power from the free stream than the Beltz limit.

1.3. Problem statement

The standard turbine selection chart in Fig. 3 illustrates how Banki turbines, which are easily manufactured using simple manufacturing techniques in small local workshops, have historically been used for rural electrification with a minimum water head of 5 m. Elbatran et al. [2] have attempted to use this affordable technology for ultra low head applications for horizontal axis by mounting one turbine on top of the other, with promising results acquired. Based on this research, it is believed that with vertical axis orientation by augmenting or guiding the water using nozzle diffuser casing could provide an affordable technically viable solution for ultra low head applications even being useful as hydrokinetic mode without the need for penstock, civil structure etc.

Cross-flow turbines are appropriate for producing power from current and waves, but the research done raises many concerns about how the cross flow turbine runner can be improved to function well in extremely low head conditions. It is advised to use standard geometrical parameters or procedures to fix the runner's size for a stream or wave current application. Two turbine runners installed vertically next to each other without an internal shaft and two separately functioning sliding guide systems with a volume flow rate of $1 \text{ m}^3/\text{s}$ and a head of less than 3 m were taken into consideration in this study. Elbatran employed the direct nozzle diffuser system for horizontal runner arrangement and modified the nozzle and diffuser arrangement in order to improve the low rotational speed of the runner, which was studied numerically around cross flow turbine [2]. Similar design vertical axis wind turbine based on the recommendation by to harness maximum energy from flowing streams, augmentation techniques can be deployed for vertical axis hydrokinetic wind turbines [6]. Conversely, the numerical study of the vertical runner orientation around cross flow turbine by direct nozzle diffuser system for vertical runner arrangement is done in this research and in Ref. [7]. Flow augmentation could solve the problem associated during the start of operation and increase the maximum power output [8]. Other turbine configurations, based on the recommendation according to Elbatran design, might result in a system that is more effective [2].

Therefore, this study intends to discover the effect of improving the speed and efficiency by using nozzle and nozzle diffuser arrangements surrounding two vertical axis cross flow turbine runners, using CFD modeling. To accelerate the fluid nozzle and two turbine runners mounted vertically side by side without internal shaft for a volume flow rate of $1 \text{ m}^3/\text{s}$ and running for head less than 3 m, and for the same geometric configuration by integrating diffuser to the system the performance effect of the diffuser also tasted through the Ansys-Fluent model separately.

2. Design of runner, distributor, and diffuser

Traditional design procedures are reviewed, and a new and more complete one is proposed to overcome the design gaps of Banki turbines, providing new expeditious equations and data to be used in practical applications. The new recent equations obtained by Ref. [9] elaborate and generalize literature and industrial data, presenting them in a dimensionless form. The current share of Banki turbines and their future developments and opportunities are also discussed. Ref. [9] and in this research, these equations are used in the design of the new vertical axis Hydrokinetic dual axis Banki turbines.

Ref. [2] in his study of the horizontal axis, hydrokinetic Banki turbines recommended that it was important to get suitable inlet and outlet angles for use in the current configuration. Hence, there is a lack of theoretical understanding on changing these angles to be suitable in his hydrokinetic applications, which is strongly manifested in all previous literature,

The complete assembly of vertical dual-axis Banki turbine with nozzle diffuser surrounding assembly the components assembled include the distributor at the entrance, nozzle, runner section, and diffuser. But for the case study without a diffuser, the same design was utilized without a diffuser studied in this research.

From literatures using the latest design procedure utilized for Banki turbine for the water running with 3 m elevation and the flow rate of $1 \text{ m}^3/\text{s}$ is studied in this research with all overall dimensions shown in Fig. 4.

$$N_s = \frac{NP_{Out}^{\frac{1}{2}}}{H_n^{1.25}} \quad (1)$$

$$N_s = \frac{513}{H_n^{0.505}} \quad (2)$$

Assuming an efficiency of 75% due to manufacturing facilities in developing nations,

Case-1

$$Q_{tot} = 1 \text{ m}^3/\text{s}$$

and half of the total flow goes to the first and the other half to the second runner.

$$Q_{1st} = 0.5 \text{ m}^3/\text{s} \text{ and } Q_{2nd} = 0.5 \text{ m}^3/\text{s}.$$

Therefore,

$$P_{Out} = \eta \rho g H_n Q \quad (3)$$

$$P_{Out,t1} = \eta \rho g H_n Q_{1st} \wedge P_{Out,t2} = \eta \rho g H_n Q_{2nd}$$

$$P_{Out,t1} = 10.4 \text{ kW} \wedge P_{Out,t2} = 10.4 \text{ kW}$$

Then the specific speed of the runner, which depends on the net head is given by the empirical formula

$$N_s = \frac{513}{H_n^{0.505}} = 303.9 \text{ rpm}$$

The runner's actual speed is given by

$$N_{t1} = \frac{H_n^{1.25} N_s}{P_{Out,t1}^{\frac{1}{2}}} = 344 \text{ rpm} \wedge N_{t2} = \frac{H_n^{1.25} N_s}{P_{Out,t2}^{\frac{1}{2}}} = 344 \text{ rpm} \quad (4)$$

$$D_1 = \frac{82.9 \times SR_{th} \times \cos \alpha \times \sqrt{H_n}}{N} = 0.188 \text{ m}$$

The Internal diameter,

$$D_2 = 0.66 D_1 = 0.124 \text{ m}$$

The inflow angle

$$\beta_1 = \tan^{-1}(2 \tan \alpha) = 39^\circ \quad (5)$$

The outflow angle is instead generally set to $\beta_2 = 90^\circ$

The depth of the water jet just upstream of the blade tip s was suggested to be:

$$s = k \cdot D_1 = 0.016 \text{ m} \quad (6)$$

The distance between two blades t is:

$$t = \frac{s}{\sin \beta_1} = 0.026 \text{ m} \quad (7)$$

The width (height) of the nozzle from the continuity equation:

For a single turbine, the flow width with clearance for environmental protection is given by

$$W = \frac{D_1}{2} + ST + CL \quad (8)$$

where W: nozzle outlet width on one side of the runner, ST: thickness of sliding gate assumed to be 6 mm thick sheet metal in this design, and CL clearance on one side of the runner assumed to be 50 mm

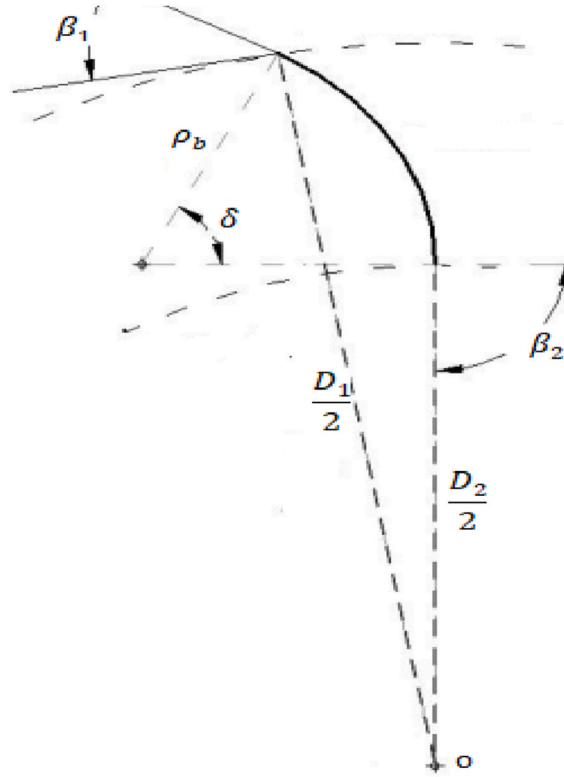


Fig. 5. Blade geometry.

$$W = 0.15m$$

The velocity of water at the inlet V

$$V = C_v \sqrt{2gH_n} = 7.3m/s \tag{9}$$

In the latest design procedure set by Ref. [2], the entry arc angle λ is fixed, typically 90° , and the nozzle dimensions are calculated. The height of the nozzle and runner of the two turbine assemblies are assumed to be equal and from continuity equation

$$b = \frac{Q_{n1}}{V \cdot W \cdot c} = 0.54m \tag{10}$$

where $C = 0.85$ is the roughness correction factor used for the smooth canal. The curvature radius of the runner blade is a function of the inlet and outlet blade angle of the runner as well as the inner and outer radius of the runner [9]. Finally, after performing the necessary calculations the blade detail profile shown in Fig. 5.

$$\rho_b = \frac{[R_1^2 - R_2^2]}{2(R_1 \cos \beta_1 + R_2 \cos \beta_2)} [m] = 0.034m \tag{11}$$

The angle of the center of the blade is given by

$$\tan \frac{\delta}{2} = \frac{\cos \beta_1 - \frac{R_2}{R_1} \cos \beta_2}{\sin \beta_1 + \frac{R_2}{R_1} \sin \beta_2} \tag{12}$$

$$\delta = 62^\circ$$

The length of the blade is given by $\rho_b \delta$.

Mockmore, and Merryfield's equation for the number of blades,

$$N_b = \frac{\pi \sin \beta_1}{k} = 22.7 \cong 23 \text{ The constant } k = 0.087 \tag{13}$$

And again from Mockmore and Merryfield, the standard blade thickness used $t_b = 3mm$.

Speed ratio $SR = U/V_U$: this is defined as the ratio of U, the blade tangential speed, to V_U , the inflow water velocity exiting the nozzle and projected along the U direction. The theoretical optimal value is $SR_{th} = 1/2$, by applying the velocity triangle theory for configuration shown in Fig. 6 and finding the maximum power

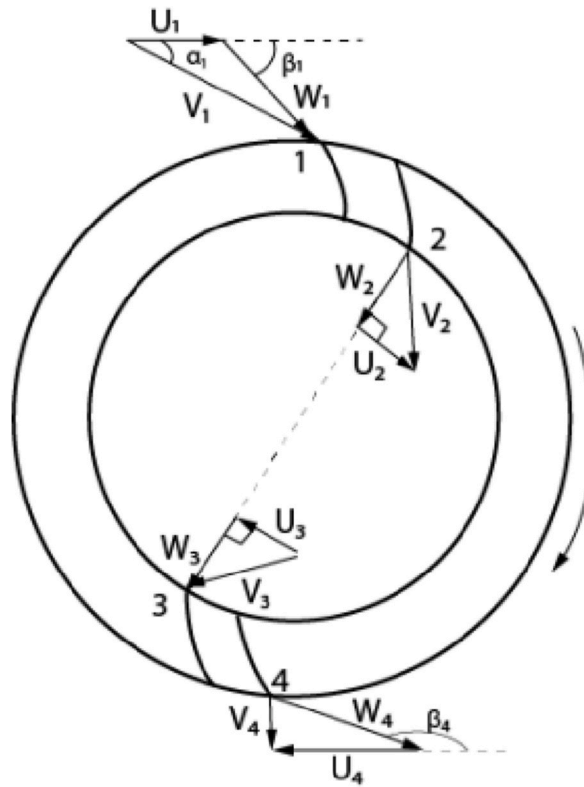


Fig. 6. Velocity triangle.

Table 2
Runner geometry.

Runner Geometry	Size
Number of Blades (Nb)	23
Inner dia. of Runner (D2)	124 mm
Outer dia. of Runner (D1)	188 mm
Inlet Blade angle (\$\beta_1\$)	39°
Outlet Blade angle (\$\beta_2\$)	90°
Angle of attack	22°
Blade radius	34 mm
Height of runner	540 mm
Blade angle	62°

$$SR = \frac{U}{V \cos \alpha} \tag{14}$$

Based on the calculations performed from equation (1) to equation (14) the runner geometries are tabulated and shown in Table 2.

3. Numerical model

In this research, a finite volume method was used for discretizing the governing equations in Ansys Fluent. Steady simulation was performed based on Reynolds averaged Navier–Stokes equations with (SST) $k-\omega$, for turbulence model. This turbulence model combines $k-\omega$ turbulence model and $k-\epsilon$ model, where $k-\omega$ turbulence model is used in the near wall region and the $k-\epsilon$ model is used in the free-stream flow. The pressure based solver with absolute velocity formulation was used, gravity and axis of rotation in the z direction considered. The fluid considered was water with y axis flow direction and density 998.2 kg/m^3 and viscosity 0.001003 kg/m.s , the turbine and wall materials are steel with density 8030 kg/m^3 , the mass flow at the inlet considered 1000 kg/s at zero gauge pressure. In the solution methods, the residual set was 0.00001 and the result converged after 394 iterations.

3D simulation for flow of incompressible viscous using RANS (Reynolds average Navier-Stokes equation) with SST $k-\omega$ turbulence model using ANSYS-Fluent.

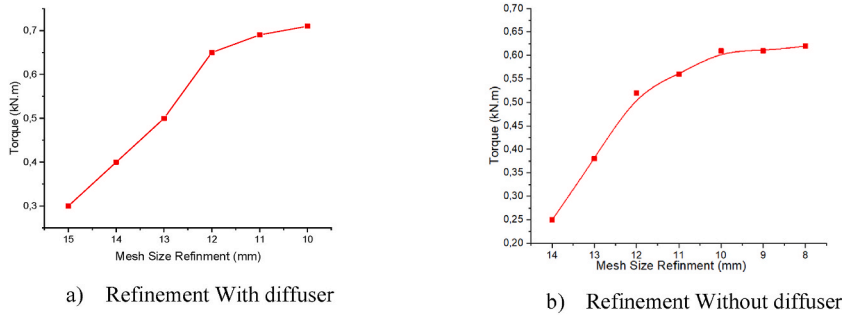


Fig. 7. Mesh sensitivity plot.

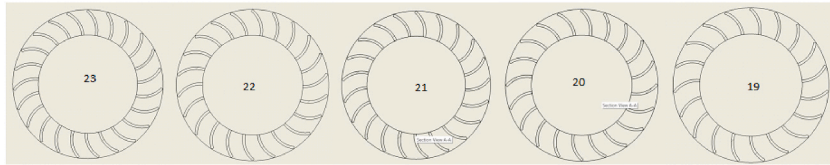


Fig. 8. Geometry Optimization by reducing the number of blades.

$$\frac{\partial u_i}{\partial x_i} = 0 \tag{15}$$

$$\rho \left(\frac{\partial u_i}{\partial t} + \frac{\partial}{\partial x} (u_i u_j) \right) = - \frac{\partial p}{\partial x_i} + \frac{\partial}{\partial x} (\overline{\rho u_i u_j}) + \frac{\partial}{\partial x_j} \left(\mu \left(\frac{\partial u_i}{\partial x_j} + \frac{\partial u_j}{\partial x_i} \right) \right) \tag{16}$$

$$-u_i u_j = \mu \left(\frac{\partial \bar{u}_i}{\partial x_j} + \frac{\partial \bar{u}_j}{\partial x_i} \right) - \frac{2}{3} k \delta_{ij} \tag{17}$$

k – ω Model

The general form for k – ε and k – ω model, Ref. [5]

$$\epsilon = C_\mu k \omega \tag{18}$$

$$\frac{\partial(\rho k)}{\partial t} + \nabla \cdot (\rho u k) = \nabla \cdot \left(\left(\mu + \frac{\mu_t}{\sigma_k} \right) \nabla k \right) + P_k - \rho \epsilon \tag{19}$$

$$\frac{\partial(\rho \omega)}{\partial t} + \nabla \cdot (\rho u \omega) = \nabla \cdot \left(\left(\mu + \frac{\mu_t}{\sigma_k} \right) \nabla \omega \right) + \frac{\gamma}{v_t} P_k - \beta \rho \omega^2 + 2(1 - F_1) \frac{\rho \sigma \omega^2}{\omega} \nabla k : \nabla \omega \tag{20}$$

$$\nabla k : \nabla \omega = \frac{\partial k}{\partial x} \frac{\partial \omega}{\partial x} + \frac{\partial k}{\partial y} \frac{\partial \omega}{\partial y} + \frac{\partial k}{\partial z} \frac{\partial \omega}{\partial z} \tag{21}$$

where F_1 is the damping function, and when $F_1 = 0$ the system uses k – ε model and when $F_1 = 1$ the damping function becomes zero and the system uses k – ω model. Every cell in the mesh do have different F_1 value.

4. Geometry optimization

The boundary conditions considered in the study at the entrance the volume flow rate of 1m³/Sec, no slip in side wall and zero static pressure at the outlet for both with and without diffuser assemblies considered. Based on Elbatran et al. [5] design procedure of Banki turbines the number of blades calculated was 23.

The mesh refinement for design with diffuser assembly and without diffuser assemblies becomes smooth for fine mesh arrangement for both cases.

CFD optimization performed in this study provides good result, as shown in Fig. 7 for 19 number of blades design, maintaining all other geometric parameters of the runner the same also shown in Fig. 8.

The optimization performed on the distributor throat dimension simulation converges for 202 mm width.

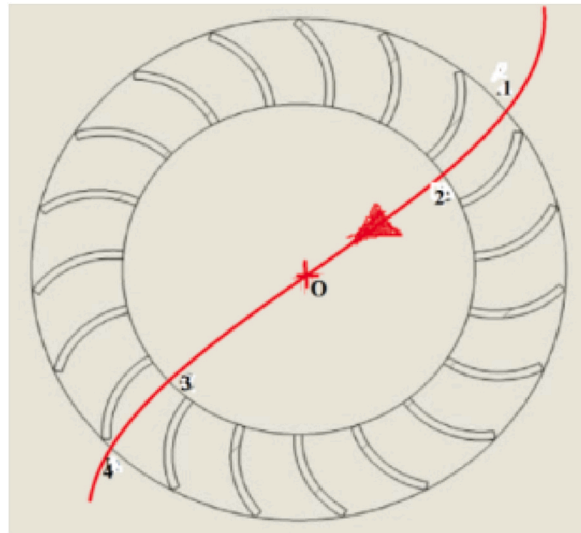
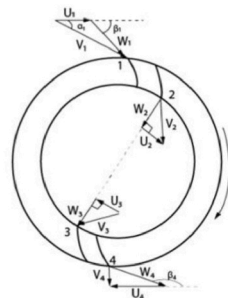


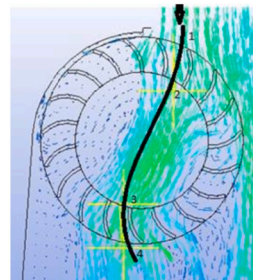
Fig. 9. Inlet outlet stages for single streamline.

$$V_1 = 9.5 \text{ m/s} \quad P_1 = 39.5 \text{ kPa} \quad V_2 = 11.5 \text{ m/s} \quad P_2 = 12.6 \text{ kPa}$$

$$V_O = 10.2 \text{ m/s} \quad P_O = -11 \text{ kPa} \quad V_3 = 10.9 \text{ m/s} \quad P_3 = -12.2 \text{ kPa} \quad V_4 = 8.5 \text{ m/s} \quad P_4 = 16.8 \text{ kPa}$$



a) Velocity triangle



b) Velocity Contour

Fig. 10. Velocity triangle for inlet and outlet stages.

$$R_{d12} = \frac{\Delta P_{PresE}}{H_e} = \frac{(U_1^2 - U_2^2) + (W_2^2 - W_1^2)}{(U_1^2 - U_2^2) + (W_2^2 - W_1^2) + (V_1^2 - V_2^2)} = 0.73 \tag{22}$$

4.1. Energy extracted in different stages

As shown in Fig. 9. The energy extracted through the inlet stage (1–2) is 66.3% and the outlet stage (3–4) is 33.7%. Due to constriction at rotor entrance, there is an increase in velocity and decrease of pressure, which results in some degree of reaction (Rd) (see Fig. 10).

5. Validation

Results of validation in relation to Elbatran et al.'s [2] hydrokinetic dual horizontal axis Banki turbine architecture The case study for this research's diffuser-free design shows a similar velocity distribution to this one, but the vertical axis assembly performs better in the diffuser-equipped design because the flow maintains a relatively uniform speed at the runner outlet the slop initially deviates by 0.5% and becomes in an acceptable range as shown in Fig. 11.

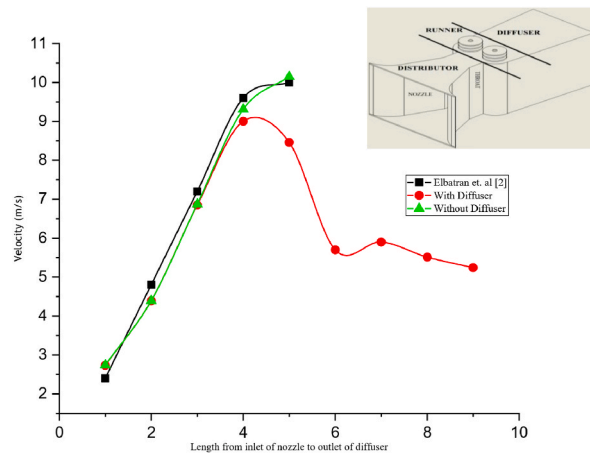
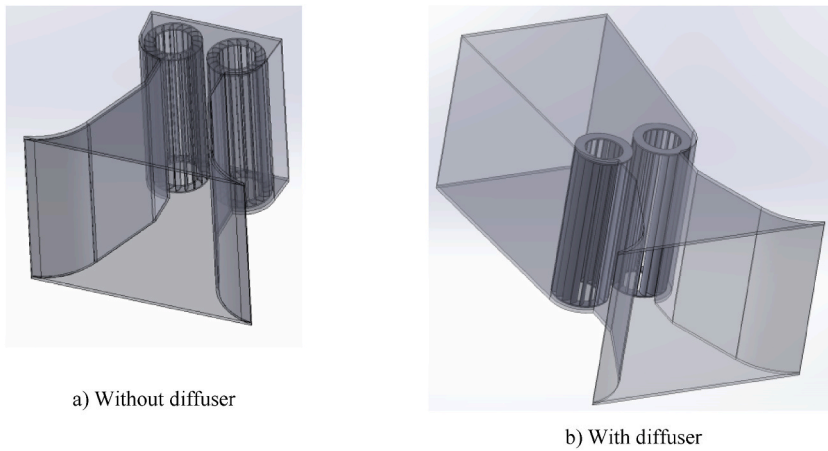


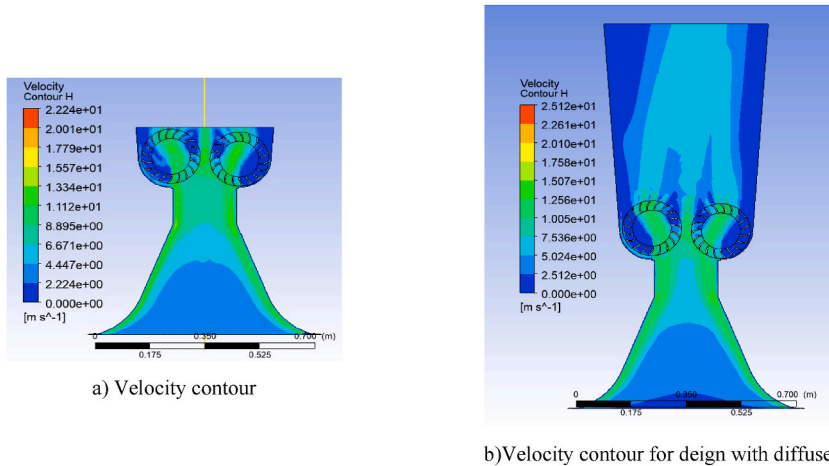
Fig. 11. Comparative velocity distribution for inlet and outlet stages for validation.



a) Without diffuser

b) With diffuser

Fig. 12. Assembly without and with diffuser.



a) Velocity contour

b) Velocity contour for design with diffuser

Fig. 13. Velocity and pressure profile on a plane at 0.448 m height from the ground.

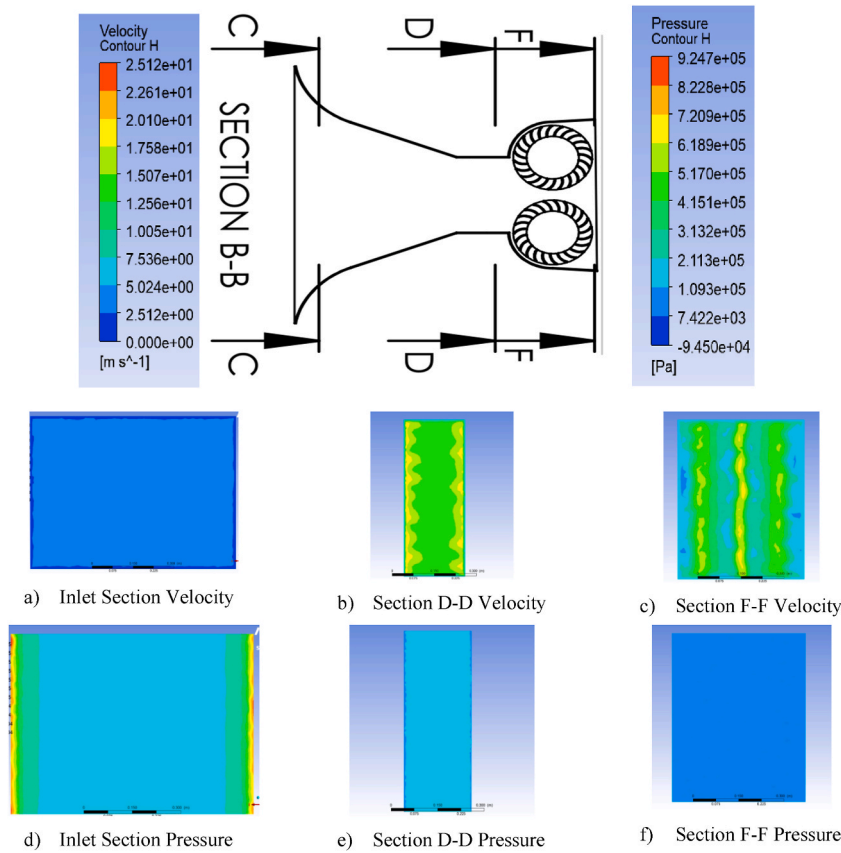


Fig. 14. Velocity and Pressure contour for assembly without the diffuser.

6. Result

The result for turbine with diffuser and without diffuser assembly shown in Fig. 12a and b respectively is presented separately in the following section.

The model generated using SolidWorks in Fig. 12 shows the optimized geometry of the design without diffuser, shown in Fig. 13a which operates somehow at lower efficiency than the one with diffuser shown in Fig. 13b the diffuser geometry helps the system recover the energy of water to be wasted. The Ansys-Fluent model for the same boundary condition for both with and without diffuser geometries shows the velocity distribution in XY plane at a height (Z) in a plane considering 60% of the height of the runner, the area average velocity contour for without diffuser design shows higher value, which still needs to be extracted, and Fig. 13b the velocity is relatively lower implies the diffuser helps to extract more energy from water. In both cases the system inputs and boundary conditions are the same and symmetrical, but the velocity contour result shows no symmetry because of the moving/floating geometry of the runners, which it cannot start operation at the same angle of attack.

The total pressure and velocity energy at any point based on Bernoulli's equation considering there is no significant elevation difference in the controlled region.

$$e_i = \frac{P}{\rho} + \frac{v^2}{2} \tag{23}$$

Figs. 14 and 15 shows the area average velocity and pressure contour in XZ plane for without diffuser and with diffuser designs respectively for Y axis flow direction with the colour contour map Fig. 14 a–f, and Fig. 15a–h, in general the pressure and flow distribution for design without diffuser is symmetrical through the Z axis, and relatively uniform as compared with the design with diffuser assembly, therefore the assembly without diffuser is more stable with lower level of vibration or water hammer effect than the design with diffuser assembly, which helps to consider reinforcement while installing the more efficient with diffuser assembly.

Considering area average velocity at different ten locations in the flow direction as shown in Fig. 16, at the outlet for design without diffuser the speed of water is much higher than with diffuser assembly, this shows there is still much hydrokinetic energy which needs to be extracted and the design with diffuser provides a system that helps recover part of the energy to be wasted.

As shown in Table 3, the inlet the energy due to speed and pressure of water for both with and without diffuser cases is 111.9 kW, but out of this energy 1.8 kW is wasted for the case with diffuser assembly and 10.9 kW for design without diffuser, which in general

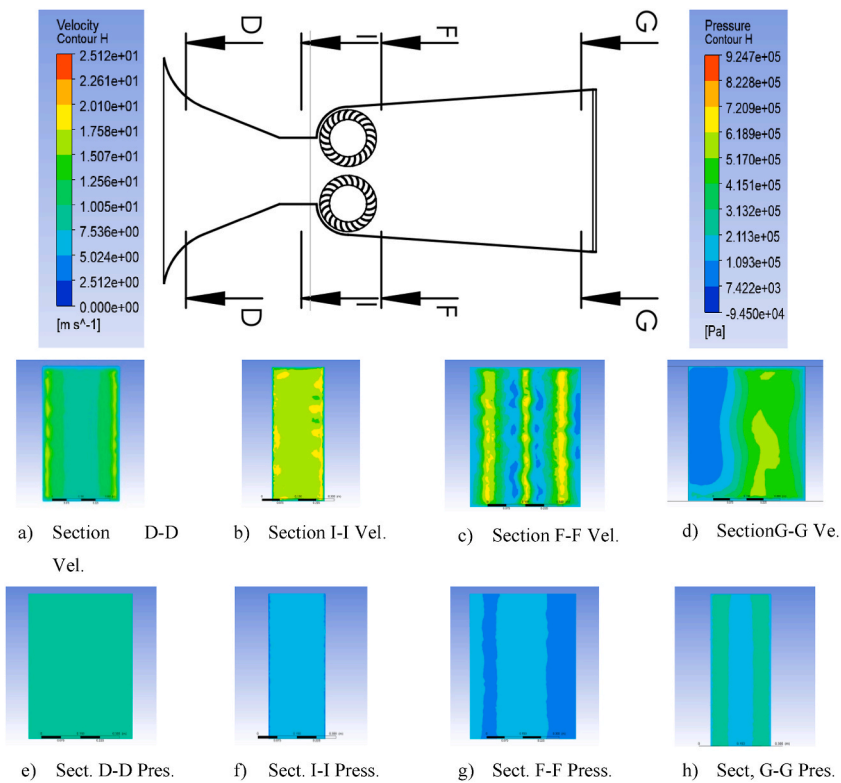


Fig. 15. Velocity and pressure contour for assembly with diffuser.

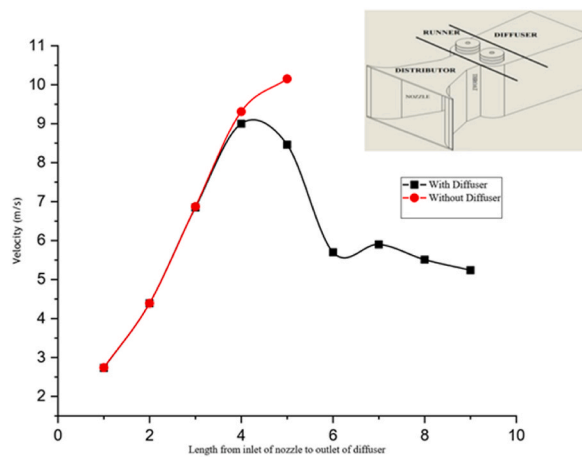


Fig. 16. Average velocity and pressure distribution for both assemblies across the length.

Table 3
Power and torque distribution.

Energy with diffuser	Power (kW)	Torque (kN.m)
Inlet (C)	111.9 kW	0.71
Distributor throat (A)	68.3 kW	
Turbine outlet (D)	1.8 kW	
Energy without diffuser		
Inlet (C)	111.9 kW	0.62
Distributor throat (A)	68.9 kW	
Turbine Outlet (B)	10.9 kW	

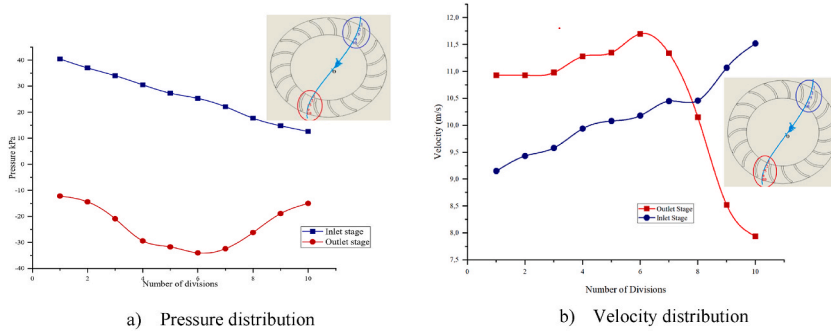


Fig. 17. Velocity and pressure distribution for inlet and outlet stages separately.

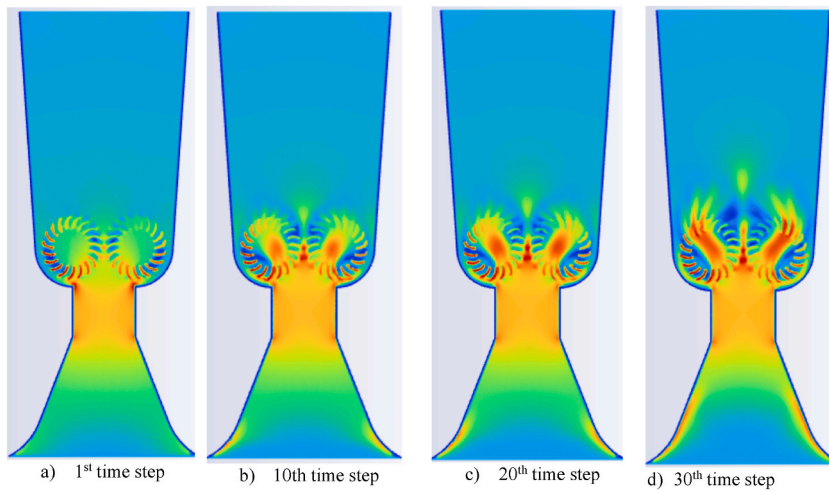


Fig. 18. Transient behavior during the start of operation.

shows 9.1 kW of energy recovered by the diffuser, and the torque value of 0.71 kN m and 0.62 kN m for with diffuser and without diffuser assemblies respectively.

A single water stream hits the runner twice that is one of the important advantage of cross flow turbine the inlet stage extracts most of the energy from water and the remaining extracted in the outlet stage. At the inlet stage the gap between two runner blades reduces and forms nozzle type of geometry, and the outlet stage forms diffuser like geometry. Fig. 17a demonstrates the pressure gradient at the inlet/nozzle and outlet/diffuser stages of the runner. The pressure almost linearly reduces with slop approximately about three, at the inlet/nozzle stage, but at the outlet/diffuser the pressure initially reduces and starts increasing. Fig. 17b shows the linear velocity increment at the inlet/nozzle stage of the runner and sharply reduces at the outlet/diffuser stage after slight initial increment. This all rate of velocity and pressure increment at the inlet and outlet stages respectively, and reduction in velocity and pressure at the outlet and inlet shows the energy extracted by the is due to this velocity and pressure changes.

6.1. Transient behaviour

The transient model demonstrates after the start of operation the flow overcomes the shear layer after the 30th time step, where the flow becomes steady, for each timestep size considered 0.001s. Fig. 18 a) shows the standard initial condition when the flow initially starts, b) and c) shows the flow development till finally becomes steady and fully developed in d) for operation of the system in general the runaway condition considered.

7. Conclusions

- In vertical axis cross flow turbines without internal shaft, efficiency of the turbine with diffuser assembly is 59.4% against 51.8% for the case without diffuser.
- The presence of diffuser enabled energy recovery at the exit to the extent of 33.7%.
- The bell mouth entrance to the throat section of diffuser and turbine significantly enhances turbine performance in terms of efficiency 4–11%.

- The optimum number of runner blades have been found to be 19 and throat width at 202 mm.
- The system incurs minimum or significantly lower initial investment as compared with the same capacity horizontal axis Banki turbine, because it doesn't require civil structures like diversion weir, forebay, powerhouse, and other complicated structures.
- Flow separation in diffuser section and some portions of the turbine runner still exists and must be further studied.

CRedit authorship contribution statement

Nebiyu Bogale Mereke: Writing – original draft, Validation, Software, Project administration, Methodology, Investigation, Formal analysis, Conceptualization. **Venkata Ramayya Ancha:** Writing – review & editing, Supervision, Methodology, Formal analysis. **Patrick Hendrick:** Writing – review & editing, Validation, Supervision, Project administration, Methodology.

Declaration of competing interest

The authors declare that they have no known competing financial interests or personal relationships that could have appeared to influence the work reported in this paper.

Acknowledgements

The authors would like to acknowledge the support from Jimma University, Jimma Technology Institute(JiT)-Center of Excellence, Jimma, Ethiopia and Université Libre de Bruxelles, Aero-Thermo-Mechanics Department during the course of this work.

References

- [1] Muluken Temesgen Tigabu, David Wood. Analytical, Computational, and Experimental Study of Vertical axis Hydrokinetic Turbines: Bahir Dar Institute of Technology School of Graduate Studies.
- [2] A.H. Elbatran, O.B. Yaakob, Yasser M. Ahmed, Ahmed S. Shehata, Numerical and experimental investigations on efficient design and performance of hydrokinetic Banki cross-flow turbine for rural areas, *Ocean Eng.* 159 (2018) 437–456, <https://doi.org/10.1016/j.oceaneng.2018.04.042>.
- [3] Daniela Popescu, Constantin Popescu, Andrei Dragomirescu, Flow control in Banki turbines, *Energy Proc.* 136 (2017) 424–429, <https://doi.org/10.1016/j.egypro.2017.10.272>.
- [4] Andrei Dragomirescu, Mihai Schiaua, Experimental and numerical investigation of a Banki turbine operating far away from the design point, *Energy Proc.* 112 (2017) 43–50, <https://doi.org/10.1016/j.egypro.2017.03.1057>.
- [5] A.B. Timilsina, S. Mulligan, T.R. Bajracharya, Water vortex hydropower technology: a state-of-the-art review of developmental trends, *Clean Technol. Environ. Policy* 20 (2018) 1737–1760, <https://doi.org/10.1007/S10098-018-1589-0>.
- [6] S.D. Karmakar, H. Chattopadhyay, A review of augmentation methods to enhance the performance of vertical axis wind turbine, *Sustain. Energy Technol. Assessments* 53 (2022) 102469, <https://doi.org/10.1016/j.seta.2022.102469>.
- [7] A.H. Elbatran, O.B. Yaakob, Yasser M. Ahmed, M. Rajali Jalal, Novel approach of bidirectional diffuser-augmented channels system for enhancing hydrokinetic power generation in channels, *Renew. Energy* 83 (2015) 809–819, <https://doi.org/10.1016/j.renene.2015.05.038>.
- [8] K.H. Wong, W.T. Chong, N.L. Sukiman, S.C. Poh, Y.C. Shiah, C.T. Wang, Performance enhancements on vertical axis wind turbines using flow augmentation systems: a review, *Renew. Sustain. Energy Rev.* 73 (2017) 904–921, <https://doi.org/10.1016/j.rser.2017.01.160>.
- [9] Emanuele Quaranta, Jean Pierre Perrier, Roberto Revelli, The optimal design process of crossflow Banki turbines: literature review and novel expeditious equations, *Ocean Eng.* 257 (2022) 111582, <https://doi.org/10.1016/j.oceaneng.2022.111582>.